X-ray analysis of the accreting supermassive black hole in the radio galaxy PKS 2251+11

S. Ronchini[1-2-3], F. Tombesi[3-4-5-6], F. Vagnetti[3], F. Panessa[7], G. Bruni[7],

[1]Gran Sasso Science Institute, Viale F. Crispi, 7 - 67100 L'Aquila, Italy; [2]INFN - LNGS, I-67100, L'Aquila (AQ), Italy; [3]University of Rome "Tor Vergata", Via della Ricerca Scientifica 1, I-00133 Rome, Italy; [4]University of Maryland, College Park, MD 20742, USA; [5]NASA/Goddard Space Flight Center, Code 662, Greenbelt, MD 20771, USA; [6]INAF-OAR, Via Frascati 33, 00078 Monteporzio Catone, Italy; [7]INAF-IAPS, via Fosso del Cavaliere 100, I-00133 Roma, Italy

Contact: samuele.ronchini@gssi.it

Introduction

Context:

Investigation of the dichotomy between jetted and non-jetted active galactic nuclei (AGNs), in order to determine the fundamental differences of these two classes in the properties of accretion onto the central supermassive black hole (SMBH), also in light of the unified model of AGNs.

Aims:

- To study and constrain the structure, kinematics and physical state of the nuclear environment in the broad line radio galaxy (BLRG) PKS 2251+11, through a detailed spectral and temporal analysis of the nuclear X-ray emission. The high X-ray luminosity and the relative proximity make such AGN an ideal candidate for a detailed analysis of the accretion regions in radio galaxies.
- Discover possible systematic differences in the X-ray properties between the BLRGs and the larger class of radio-quiet Seyfert galaxies.

Methods:

We performed an X-ray spectral and timing analysis of a ~64 ks observation of PKS 2251+11, taken with the instrument EPIC-pn on board of XMM-Newton. We modeled the spectrum considering an absorbed power law superimposed to a reflection component. We performed a time-resolved spectral analysis to search for variability of the X-ray flux and of the individual spectral components.

The Unified Model of AGNs

COMMON INGREDIENTS

- (a) Central SMBH
- (b) Accretion disk
- (c) Obscuring torus
- Nuclear outflows → crucial for AGN feedback
  - (d) Relativistic radio jet → present only in ≃10% of AGNs
  - (e) Disk winds → present in both Radio Loud and Radio Quiet AGNs, hence independent on the presence of the radio jet

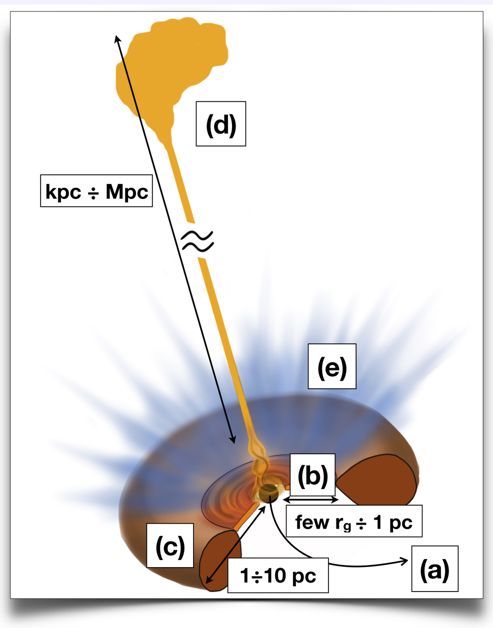

MAIN OPEN QUESTIONS:

- Can a single unified model explain the complexity of AGNs families?
- How the accretion physics is connected to the outflow mechanisms?
- Are the structure and the geometry of the circum-nuclear environment somehow related to the production of outflows?
- Is there a defined difference between jetted and non-jetted AGN in the accretion properties, somehow connected to the presence or not of nuclear outflows? → Different physical state of the accretion disk (ADAFs vs geometrically thin disks), accretion rate and efficiency, bolometric luminosity, mass and spin of the SMBH?

Advantages of BLRGs

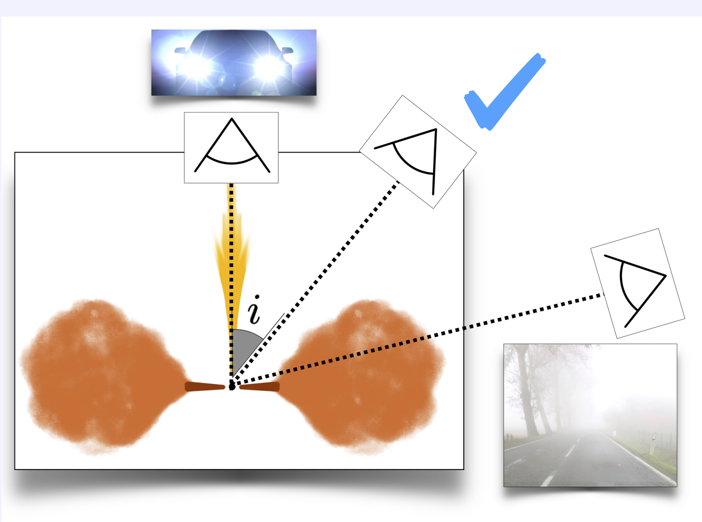

The inclination angle between the line of sight and the perpendicular to the equatorial plane has an intermediate value between 0° and 90°. Hence, the X-ray radiation emitted in the proximity of the SMBH is

- neither suppressed by the obscuring torus
- nor overwhelmed by the relativistically boosted emission of the jet, as in blazars

⇓

We are able to study directly the properties of the innermost nuclear regions

Tab 1: Quick facts about PKS 2251+11

Parameter	Value	Units	notes
redshift z	0.33	-	
M_{BH}	$7-17$	$10^8\ M_\odot$	
$\log[\eta \dot{M} c^2/L_{Edd}]$	-1.5	-	(a)
$\dot{M}$	$\simeq 1-4$	$M_\odot$/yr	
L_{Edd}	$\simeq 1.4$	10^{46} erg/s	(b)
L_X	1.15	10^{44} erg/s	(c)
$\log R$	2.56	-	(d)
i	67°	-	(e)

(a) η is the accretion efficiency and $\dot{M}$ the accretion rate. (b) Eddington luminosity. (c) X-ray luminosity in the energy range E=0.2-20 keV. (d) radio loudness, equivalent to $R = 1.36 \times 10^5 L_5/L_B$, with $L_5 = L_\nu|_{\nu=5\text{ GHz}}$ and $L_B = L_\nu|_{\nu=4400\text{Å}}$. (e) angle between the jet direction and the l.o.s.

Components of AGN X-ray spectrum

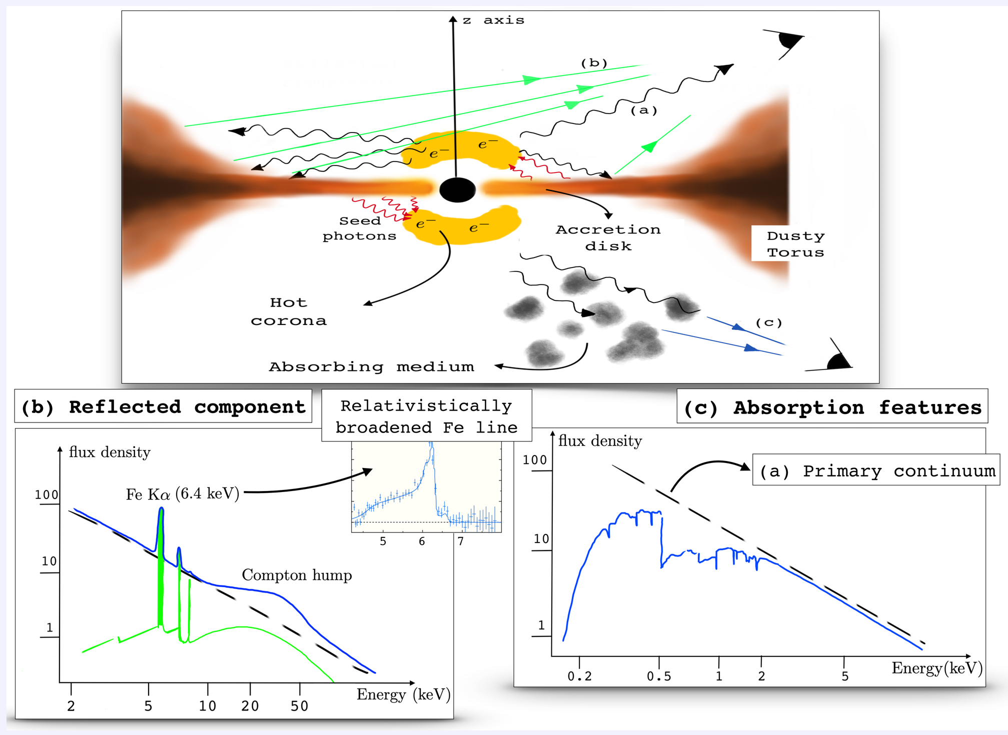

Spectral analysis

Modeling

We followed the standard assumption that the X-ray continuum is dominated by the presence of a hot corona, which comptonizes the seeds photons coming from the accretion disk. The primary continuum can be reprocessed through absorption and/or reflection, due to the surrounding environment.

Power law + neutral total covering absorber — XSPEC syntax: `ztbabs*zpo`

Power law + neutral partial covering absorber — `zpcfabs*tbabs*zpo`

Absorption in the proximity of the AGN

Absorption due to ISM in our Galaxy

$\frac{\chi^2}{d.o.f.} = 2.49$ → Introducing the covering fraction → $\frac{\chi^2}{d.o.f.} = 1.22$

$$f = \frac{\Delta\Omega_{abs}}{\Delta\Omega}$$

$f = 1$ $\qquad$ $f < 1$

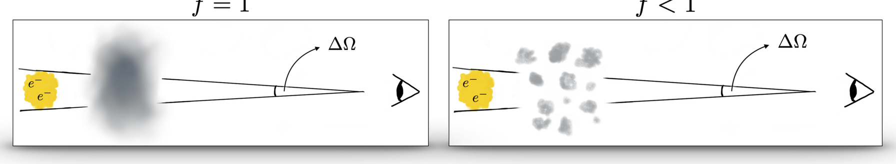

Supposing that the absorber is ionized

Best fit model:
Power law + ionized partial covering absorber + Fe Kα line modeled with a Gaussian profile

`zxipcf*tbabs*(zpo+zga)` $\frac{\chi^2}{d.o.f.} = 1.05$

The best fit model is given by:

$$S(E) = [fA(N_H,\xi,E) + (1-f)] \times [C(E) + G(E)]$$

$$C(E) = N_\Gamma E^{-\Gamma}$$

Gaussian

$$G(E) = N_{ga}\frac{1}{\sqrt{2\pi}\sigma}\exp\left(-\frac{(E-E_{ga})^2}{2\sigma^2}\right)$$

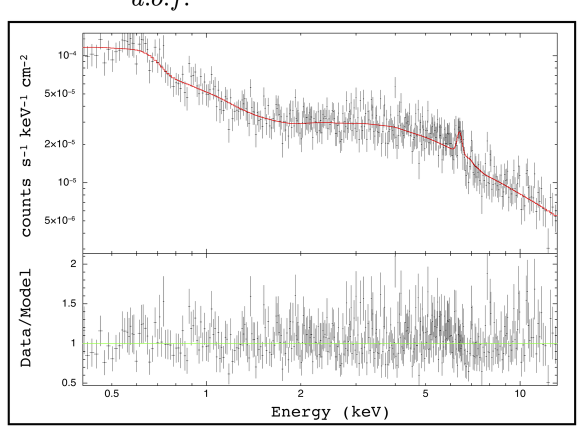

$A(N_H,\xi,E)$ is the absorption function, which depends on:

→ $N_H = \int_{l.o.s.} n(s)\,ds$ with $n(s)$ the number density of the absorbing medium

→ $\xi = \frac{L_{\rm ion}}{n(R_{in})R_{in}^2}$ with $L_{\rm ion} = \int_{13.6\ \rm eV}^{13.6\ \rm keV} L_\nu\,d\nu$

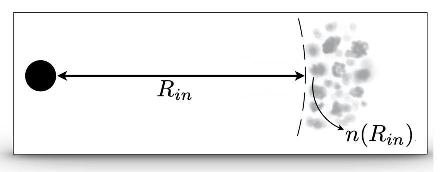

Tab 2: Best fit parameters

Parameter	Value	Units	notes
N_H	10.1 ± 0.8	10^{22}cm^{-2}	
$\log\xi$	$1.33^{+0.08}_{-0.06}$	erg s^{-1} cm	
f	0.88 ± 0.01	-	
Γ	1.78 ± 0.05	-	
E_{ga}	6.41 ± 0.03	keV	
σ	≤ 120	eV	(a)
$F^{\rm unabs}_{0.5-10\,keV}$	$2.5^{+0.1}_{-0.2}$	10^{-12}erg cm^{-2}s^{-1}	(b)
$[F^{\rm unabs} - F^{\rm abs}]/F^{\rm unabs}$	47%	-	
$L^{\rm int}_{0.5-10\,keV}$	(8.1 ± 0.5)	10^{44} erg s^{-1}	(c)
$L_{\rm ion}$	$1.24^{+0.17}_{-0.15}$	10^{45}erg/s	(d)
R	$0.64 - 1.85$	-	(e)

(a) σ is the Fe Kα line width, as written in the expression $G(E)$; since we have only an upper limit for σ, the line is not resolved. (b) flux emitted by the primary continuum without considering the suppression due to absorption. (c) Intrinsic luminosity derived from $F^{\rm unabs}_{0.5-10\,keV}$. (d) Ionizing luminosity between 13.6 eV and 13.6 keV, assuming a power law with the same Γ reported above. (e) The Fe Kα line can be fitted also using the `pexmon` model, where $R = \Omega/2\pi$ is the fraction of the solid angle covered by the reflecting medium.

Discussion

Location of the absorber: if we call $\Delta r = \alpha r$ the thickness of the absorber (with α an unknown constant), n its average number density, we can write $N_H \simeq n\Delta r$ and therefore $\xi = L_{\rm ion}/(nr^2) \simeq \alpha L_{\rm ion}/(N_H r)$

$$\Rightarrow \quad r = \alpha L_{\rm ion}/(\xi N_H) \simeq 150\alpha\left(\frac{L_{\rm ion}}{10^{45}\rm erg/s}\right)\rm pc.$$

Moreover, knowing the Hβ FWHM [4], we can estimate the location of the broad line region (BLR) as $r_{BLR} \sim GM_{BH}/v^2_{BLR} \sim 0.2$ pc, which is comparable with the distance of the absorber taking $\alpha \sim 10^{-3}$. We can also alternatively write the absorber distance as

$$r = 0.22\left(\frac{n}{10^8\ \rm cm^{-3}}\right)^{-1/2}\left(\frac{L_{\rm ion}}{10^{45}\rm erg/s}\right)^{1/2}\rm pc.$$

If we consider a density $n = 10^9$ cm^{-3}, typical of the BLR clouds (e.g. [3]), the distance of the absorber is $r \sim 0.1$ pc, again consistent with the location of the BLR.

Location of the reflector: exploiting the correlation between the centroid of the Fe Kα line and the ionization level of the reflecting material studied by [1], we can infer an upper limit for ξ_R (ionization parameter of the reflector) and consequently a lower limit for the distance of the reflector r_R from the SMBH:

$$r_R > 35\alpha\sqrt{\lambda\frac{n_A}{n_R}}\left(\frac{L_{\rm ion,A}}{10^{45}\rm erg\ s^{-1}}\right)r_A$$

where the subscript "A" refers to the absorber, "R" to the reflector and λ takes into account that the ionizing luminosity can be different for the absorber and the reflector. Moreover, under the assumption that the width of the Fe Kα line is due to Doppler broadening, an alternative estimate of r_R can be found using the upper limit $\sigma_{ga} \lesssim 120$ eV, obtaining $r_R > r_{in}$ and $600\,r_s \lesssim r_{in} \lesssim 900\,r_s$ (having assumed $50° < i < 70°$ and indicating $r_s = 2GM_{BH}/c^2$).

Time resolved spectral analysis

In order to test the variability of the individual spectral components, we computed the hardness ratio as $HR(t) = C_{5-10\ \rm keV}(t)/C_{0.5-2\ \rm keV}(t)$, where $C_{5-10\ \rm keV}(t)$ and $C_{0.5-2\ \rm keV}(t)$ are the hard and soft light curves, respectively (fig. a). Then we analyzed the intervals A, B and C separately, where the last two show a larger value of HR. No spectral parameter changes significantly, apart the intensity of the Fe Kα line, which appears to be larger in B (fig. b).

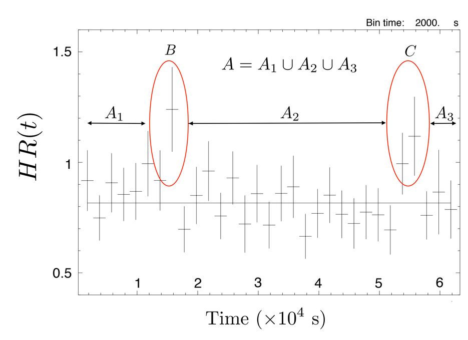

Fig. (a): temporal trend of the hardness ratio

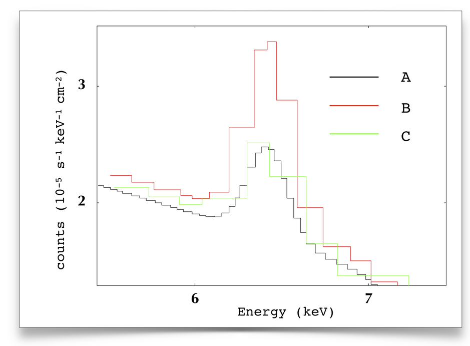

Fig. (b): Intensity of the Fe Kα line in A, B and C

Discussion

The intensity of the Fe Kα line changes in response to the variations of the incoming X-ray flux above ~7 keV. Therefore, we have proposed two scenarios to explain the variability of the reflection component:

1) Compton thick clouds rapidly moving near the X-ray primary source intercept the flux directed to the reflector

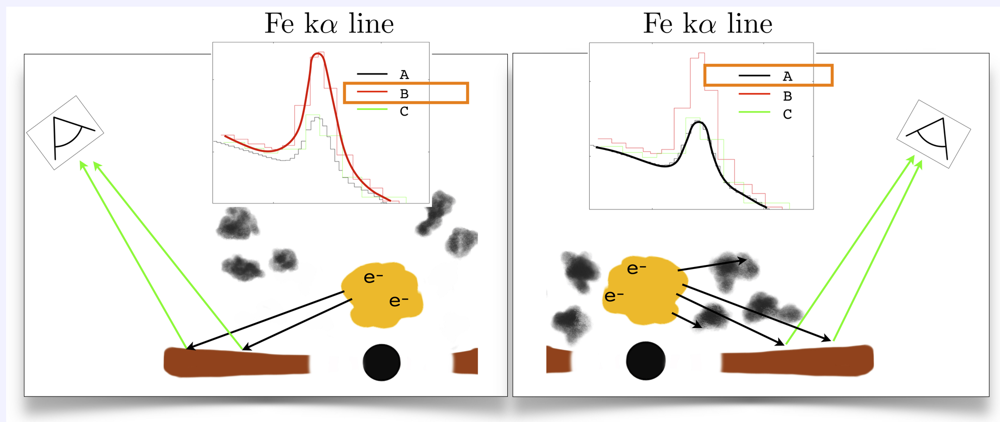

2) Since the reflector is located beyond a certain distance R_{in} from the center, there is a net time lag between the arrival time of the primary continuum and the reflected component → the primary source luminosity was variable in the past and we see the effects only now observing the reflected component.

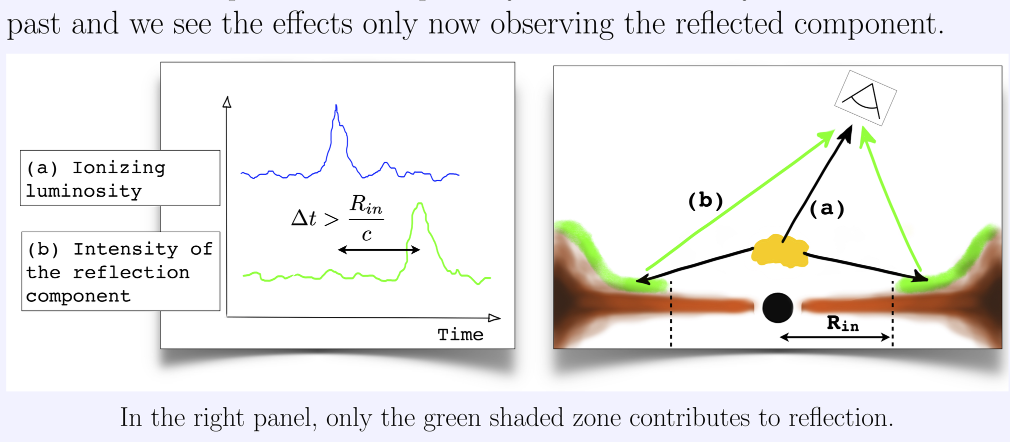

In the right panel, only the green shaded zone contributes to reflection.

Conclusions and future work

Concerning the X-ray properties, we found that PKS 2251+11 does not differ significantly from the non-jetted AGNs, confirming the validity of the unified model in describing the inner regions around the central SMBH. The absorber, likely clumpy and ionized, is compatible with the BLR or the inner zone of the dusty torus. A weak Fe Kα emission line is found at 6.4 keV, whose intensity shows variability on timescales of hours.
The X-ray analysis could be completed studying the high-energy part of the spectrum with NuSTAR, where the contribution of the jet could emerge. On the other hand, a multi-epoch X-ray monitoring can confirm or not a delayed response between the primary continuum and the reflected component, further constraining the location of the reflector. This work has been published on A&A [2].

References

[1] G. Matt, A. C. Fabian, and R. R. Ross. Iron K-alpha lines from X-ray photoionized accretion discs. *MNRAS*, 262:179–186, May 1993.

[2] S. Ronchini, F. Tombesi, F. Vagnetti, F. Panessa, and G. Bruni. X-ray analysis of the accreting supermassive black hole in the radio galaxy PKS 2251+11. *Astronomy and Astrophysics*, 625:A26, May 2019.

[3] S. A. Snedden and C. M. Gaskell. The Effect of Abundance Variations on Estimates of the Densities of Broad-Line Region Clouds in Quasars. *ApJ*, 521:L91–L94, August 1999.

[4] M. Vestergaard. Determining Central Black Hole Masses in Distant Active Galaxies. *ApJ*, 571:733–752, June 2002.